

Contents list available at the IJRED website

## **International Journal of Renewable Energy Development**

Journal homepage: https://ijred.undip.ac.id



Research Article

# Free hydrogen-deoxygenation of waste cooking oil into green diesel over Ni-Marble waste catalyst: Optimization and economic analysis

Didi Dwi Anggoro<sup>a</sup>, Didik Prasetyoko<sup>b</sup>, Hartati<sup>c</sup>, Zaki Yamani Zakaria, Brilliant Umara Le Monde<sup>a</sup>, Maulida Nurdiani

**Abstract.** Diversifying energy through alternative sources, such as biofuels, is a practical and accessible option in Indonesia. This study aimed to optimize the yield of biofuel (green diesel) using Ni/marble waste as a catalyst. Deoxygenation offers a promising route for converting waste cooking oil (WCO) into valuable products. A Box-Behnken Design (BBD) was applied to assess the effects of key variables on the deoxygenation process using Response Surface Methodology (RSM). The variables included reaction time (2–6 h), reaction temperature (360–380 °C), and catalyst weight (1–3% w/w), with conversion percentage as the response. The results showed that reaction time and catalyst weight significantly influenced WCO deoxygenation (p < 0.05). The optimum conditions for maximum conversion were a reaction temperature of 373.64 °C, a catalyst weight of 3.45% w/w, and a reaction time of 4.35 h. Under these conditions, hydrocarbon selectivity reached 92.26%. Paraffins were the dominant fraction, confirming that the Ni/marble catalyst efficiently promoted deoxygenation with high selectivity toward C15–C18 hydrocarbons. These findings align with the proposed reaction mechanism, which involves decarboxylation, decarbonylation, and hydrodeoxygenation pathways. An economic evaluation under optimal conditions estimated a profit of \$1.0469 per batch, demonstrating that converting waste cooking oil into green diesel is both technically feasible and economically attractive. Overall, integrating waste-derived catalysts with optimized deoxygenation technology provides a sustainable and profitable solution.

Keywords: Deoxygenation, Marble Waste, Optimization, Technoeconomic, Waste Cooking Oil



@ The author(s). Published by CBIORE. This is an open-access article under the CC BY-SA license (http://creativecommons.org/licenses/by-sa/4.0/).

Received: 21st March 2025; Revised: 18th July 2025; Accepted: 18th Sept 2025; Available online: 10th Oct 2025

#### 1. Introduction

The primary source of global energy production has long been fossil-based resources, which predominantly supply worldwide consumption. In recent decades, however, pressing challenges such as environmental degradation, climate change, and the depletion of fossil fuel reserves have intensified the search for sustainable alternatives. Within this context, the production of green fuels, such as green diesel, has emerged as a promising solution to mitigate the adverse impacts of petroleum-based fuels. Green diesel, or renewable diesel, shares a molecular structure like petroleum diesel and can be produced from triglycerides, free fatty acids (FFAs), and their derivatives by removing oxygen atoms from oxygenated molecules to obtain alkane hydrocarbons (Hongloi et al., 2022). The removal of oxygen, known as deoxygenation, is a crucial step in green diesel production, as high oxygen content reduces fuel quality. process involves hydrodeoxygenation (HDO). decarbonylation (DCO), and decarboxylation (DCO2) (Asikin-Mijan et al., 2016).

Second-generation or green diesel is derived from nonedible oils (Peters *et al.*, 2024), including energy crops, municipal waste, organic waste, waste vegetable oil, triolein (Kubicka, 2019), waste cooking oils (Chiaramonti *et al.*, 2016), and animal fats (Aliana-Nasharuddin *et al.*, 2019). Among these, waste cooking oil (WCO) shows strong potential for conversion into sulfur-free and nitrogen-free liquid biofuels and oxygenated chemicals. Its molecular structure resembles that of gasoline and diesel, enhancing its value for liquid fuel production (Hafriz *et al.*, 2021). Additionally, WCO helps address waste disposal challenges without competing with food sources (Hafriz *et al.*, 2018). A prominent strategy is the conversion of WCO into green diesel via deoxygenation processes catalyzed by heterogeneous systems (Reza *et al.*, 2023).

In general, reducing oxygen content (deoxygenation or DO) in FFAs can be achieved through three primary pathways: HDO, DCO, and DCO<sub>2</sub>. These reaction pathways are defined as follows:

Hydrodeoxygenation (HDO):

$$R-COOH + 3H_2 \rightarrow R-CH_4 + 2H_2O \tag{1}$$

Decarbonylation (DCO):

$$R-COOH \rightarrow R'-H \text{ (Alkenes)} + CO + H_2O$$
 (2)

<sup>&</sup>lt;sup>a</sup> Department of Chemical Engineering, Faculty of Engineering, Universitas Diponegoro, Semarang, 50 275, Indonesia

b Department of Chemistry, Faculty of Science and Data Analytics, Institut Teknologi Sepuluh Nopember, Keputih, Sukolilo, Surabaya, 60111, Indonesia

<sup>&</sup>lt;sup>c</sup> Department of Chemistry, Faculty of Science and Technology, Universitas Airlangga, Campus C UNAIR, Mulyorejo, Surabaya, Indonesia

<sup>&</sup>lt;sup>d</sup> Faculty of Chemical and Energy Engineering, Universiti Teknologi Malaysia, 81310, Skudai, Johor, Malaysia

<sup>\*</sup> Corresponding author Email: anggorophd@gmail.com (D.D.Anggoro)

Decarboxylation (DCO<sub>2</sub>):

$$R-COOH \rightarrow R-H \text{ (Alkanes)} + CO_2$$
 (3)

HDO, an exothermic reaction, produces linear alkanes with chain lengths equivalent to the initial fatty acids under high pressure in a  $\rm H_2$  atmosphere, with water ( $\rm H_2O$ ) as a by-product (Doliente *et al.*, 2020). In contrast, DCO involves elimination of the carbonyl group via cleavage of carbon–carbon (C=C) and carbon–oxygen (C=O) bonds, releasing carbon monoxide (CO). DCO<sub>2</sub> entails removal of the carboxylic group through carbon–carbon (C=C) cleavage, releasing carbon dioxide (CO<sub>2</sub>). Both DCO and DCO<sub>2</sub> are endothermic, producing shorter-chain alkenes and alkanes than the original fatty acids, along with CO or CO<sub>2</sub> and  $\rm H_2O$  as by-products (Scaldaferri & Pasa, 2019).

Reaction pathways for WCO-based green diesel have been widely studied (Fig. 1). Oxygen atoms in carboxyl groups may be removed with or without  $H_2$ . Direct elimination without  $H_2$ , known as  $DCO_2$ , yields heptadecane (n- $C_{17}$ ) and  $CO_2$  (step (m)). Alternatively, saturated fatty acids may form aldehyde compounds with  $H_2$ . Oxygen removal from aldehydes can then occur via DCO and/or HDO (Sousa *et al.*, 2018). In the DCO pathway, oxygen atoms in carboxaldehyde groups are released as CO (step (b)). In the HDO pathway, aldehydes are first converted to alcohols (step (c)), followed by oxygen removal as  $H_2O$  (steps (d) $\rightarrow$ (e)).

A strategic approach in renewable liquid fuel production is WCO conversion into green diesel through deoxygenation. WCO typically contains high levels of free fatty acids, such as oleic acid, with carboxyl groups rich in oxygen (Siraj & Ceylan, 2025). This high oxygen content leads to low heating values, thermal instability, and corrosiveness, limiting compatibility with conventional diesel engines. Deoxygenation is therefore critical for selectively removing oxygen (Sowe *et al.*, 2022). However, a major challenge lies in designing catalysts capable of achieving high conversion while maintaining selectivity for long-chain saturated hydrocarbons (C16–C18), the dominant fraction of green diesel.

Earlier studies demonstrated the importance of catalyst selection. A primary Ni/Al $_2$ O $_3$  catalyst efficiently converted used cooking oil (UCO) into C $_{15}$ –C $_{18}$  hydrocarbons but showed a slight performance decline over time. The addition of Cu produced a Ni–Cu/Al $_2$ O $_3$  catalyst with more stable and superior performance, maintaining high deoxygenation activity and low cracking activity, consistently yielding saturated C $_{15}$ –C $_{18}$  alkanes, which align with diesel characteristics (Silva *et al.*, 2020). Deoxygenation using a CaCO $_3$ /HY catalyst also showed strong performance in transforming palm oil. The synergy of HY zeolite's Brønsted acidity with CaCO $_3$ 's basicity improved product selectivity and deoxygenation efficiency, producing over 94% hydrocarbons while reducing oxygen content to 0.05% (Febriansyar *et al.*, 2023).

Transition metal-based catalysts, such as nickel (Ni), hold strong potential for FFA deoxygenation. Efficiency is influenced by catalyst structure, including the number of active sites, surface area, reducibility, and acidity. Catalysts with high active site density, easy NiO reduction, and balanced acidity offer optimal selectivity for diesel-range hydrocarbons (C16–C18), achieving 96.7% conversion and 45.9% selectivity (Jeon *et al.*, 2022). Acid–base properties are critical in enhancing deoxygenation performance. Studies confirm that regulating active metal content in heterogeneous catalysts not only improves conversion efficiency but also favors the HDO pathway, which is more environmentally friendly due to H<sub>2</sub>O as the by-product. Green diesel has also been produced from rapeseed oil using NiMoAl catalysts synthesized from layered

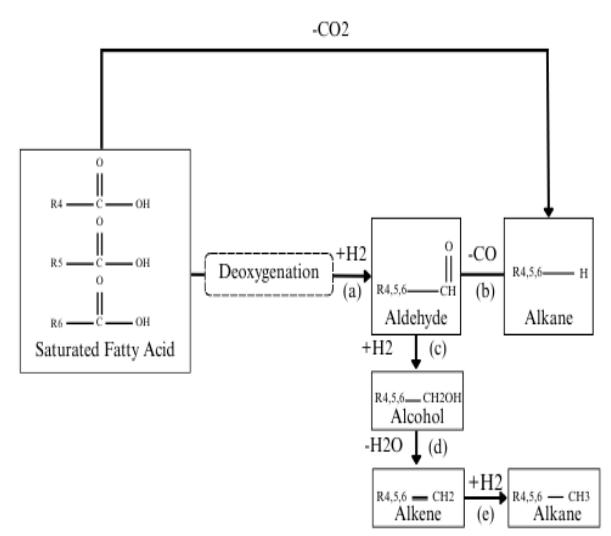


Fig 1. Reaction pathways of green diesel production from waste cooking oil

double hydroxides (LDHs) via co-precipitation. Under optimized parameters (320 °C, 40 bar  $\rm H_2$ , 4 wt% catalyst loading), the system achieved over 90% selectivity for diesel-range hydrocarbons (n-C<sub>15</sub>–C<sub>18</sub>) and maintained stability across multiple cycles, underscoring its potential for renewable diesel production (Nolfi *et al.*, 2025). Excessive catalyst acidity, however, can lead to coke formation, reducing catalyst stability and lifetime (Krobkrong *et al.*, 2018). This issue is particularly problematic with WCO feedstock, which is inhomogeneous and often contaminated with heavy metals and water. Thus, catalyst formulations balancing active sites, reducibility, and acidity are essential to optimize WCO deoxygenation efficiently and sustainably.

To optimize the deoxygenation process, it is necessary to examine the effect of process variables on the response, specifically the conversion of WCO. This study employed a three-factor Box–Behnken Design (BBD), a type of design of experiment (DOE) within response surface methodology (RSM). The aim of this study was to evaluate the effects of three operational variables—reaction time, reaction temperature, and catalyst weight—on the deoxygenation process. The study also sought to identify the most significant variable and determine the optimal operating conditions.

#### 2. Materials and Methods

The WCO used in this study was collected from a local food stall in Central Java, Indonesia. The oil had primarily been used for deep frying and had undergone repeated heating cycles, typically four times per day over three consecutive days before being discarded. Marble waste was obtained from Tulungagung, sieved to a uniform size of 60 mesh, and stored in a closed container at room temperature. Demineralized water was obtained from Dipopure, and nickel (II) nitrate from Merck was used as received. Pure nitrogen gas (99% ultra-high purity) was provided by PT. Samator Indonesia.

## 2.1 Waste Cooking Oil

The WCO used in this research was collected from a local food stall in Semarang and filtered before use. Its fatty acid composition was analyzed by Gas Chromatography–Mass

**Table 1**Process Independent Variable Range

Variable		Variable Code			Response
	Code	-1	0	+1	
Reaction Time (hour)	$X_1$	2	4	6	
Reaction Temperature (°C)	$X_2$	360	370	380	Conversion
Catalyst Weight (% w/w)	$X_3$	1	3	6	Conversion

Spectrometry (GC–MS) using a DB-5MS capillary column (30 m  $\times$  0.25 mm  $\times$  0.25 mm, Agilent Technologies).

## 2.2 Catalyst Preparation

Catalyst synthesis was performed by the incipient wetness impregnation method using Ni(NO<sub>3</sub>)<sub>2</sub>·6H<sub>2</sub>O as the metal precursor. The salt was weighed as required and dissolved in 10 mL of distilled water, then stirred for 15 min. The supporting solid (marble waste) was weighed and added to the solution, then stirred at 80 °C until a slurry formed. The slurry was dried at 60 °C for 12 h, followed by calcination at 550 °C for 5 h in an air atmosphere at a heating rate of 2 °C/min.

#### 2.3 Catalyst Characterization

The Ni/marble waste catalyst was characterized using X-ray diffraction (XRD) with a PHILIPS XPert MPD diffractometer, employing Cu  $K\alpha$  radiation at 30 mA and 40 kV, and scanned from  $5^{\circ}$  to  $80^{\circ}$  with  $0.020^{\circ}$  step increments. Textural properties were determined by  $N_2$  adsorption–desorption on a Quantachrome Touchwin v1.11 instrument, and pore size distribution was calculated with a Quantachrome ASiQwin system. The surface area was calculated using the Brunauer–Emmett–Teller (BET) method, and pore size distribution was obtained using the Barrett–Joyner–Halenda (BJH) method.

#### 2.4 Product Characterization

Deoxygenated products were analyzed for chemical composition using GC–MS. A 0.1 mL liquid sample was injected through the port into the column. Mass spectrometry was conducted with the electron impact method. The sample interacted with the stationary phase, was carried to the detector, and produced a chromatogram through the computer system. The results were compared with standard databases.

## 2.5 Process Variable Optimization

The deoxygenation of WCO was conducted in a 100 mL three-necked flask connected to a distillation setup and equipped with a stirred heating mantle. Catalyst (1–6% w/w) was added to 10 g of WCO, then purged with  $N_2$  to create an inert environment. The mixture was stirred and heated to 360–380 °C and maintained for 2–4 h under a constant  $N_2$  flow of 20 cc/min. Statistical analysis was performed with Statistica software 6.0. RSM with a BBD consisting of three factors, one block, and fifteen trials was applied to determine significant parameters and to identify optimum deoxygenation conditions for converting WCO into green diesel. The independent variables were reaction time ( $X_1$ ), reaction temperature ( $X_2$ ), and catalyst weight ( $X_3$ ). The variable ranges and RSM experimental design are presented in Table 1.

The data were analyzed using analysis of variance (ANOVA) and response surface analysis to establish functional relationships between process variables and the response. A second-order polynomial regression equation described the significance of the correlation between independent variables and conversion. The polynomial model is expressed as follows.

$$Y = \beta_0 + \sum_{i=1}^k \beta_i X_i + \sum_{i=1}^k \beta_{ii} X_i^2 + \sum_{i=1}^k \sum_{j=i+1}^k \beta_{ij} X_i X_j$$

Notes: 1) Y represents the expected response; 2)  $\beta_0$  represents a constant coefficient; 3)  $X_i$  and  $X_j$  represent independent variables; 4) k represents the number of independent variables; and 5)  $\beta_i$ ,  $\beta_{ii}$ , and  $\beta_{ij}$  represent the linear, quadratic, and interaction coefficients, respectively. The use of RSM in the experimental process reduced the number of trials required to optimize the system and response, making the optimization process more efficient and cost-effective.

## 3. Results and Discussion

## 3.1 Waste Cooking Oil Characterization

The characteristics of WCO were analyzed by GC-MS to determine its triacylglycerol (TAG) composition. The results showed that triglycerides were the dominant component (77%), followed by diglycerides (7%) and monoglycerides (5%). These findings are consistent with an earlier study that reported triglycerides as the main component of crude palm oil (74.2%) (Choo *et al.*, 2020). During deoxygenation, TAG undergoes hydrolysis, forming fatty acids and glycerol, which are then subjected to DCO<sub>2</sub> and DCO reactions. The fatty acid composition of WCO, presented in Table 2, is dominated by C16-C18 chains, with oleic acid (C18:1) being the most abundant. This composition is significant for deoxygenation pathways, as long-chain C18 fatty acids with a single double bond are easily hydrogenated into saturated species and

**Table 2**Fatty Acid Composition of Waste Cooking Oil

Fatty Acid Chain	Composition (%)
C <sub>14</sub>	1.28
$C_{16:0}$	11.7
C <sub>18:0</sub> (Stearic Acid)	4.21
C <sub>18:1</sub> (Oleic Acid)	42.27
C <sub>18:2</sub> (Linoleic Acid)	4.21
Other	36.33

subsequently deoxygenated into long-chain paraffins (C17–C18). The high percentage of triglycerides (58.17%) is favorable, indicating that the feedstock contained substantial energy-rich components convertible to hydrocarbons. Triglycerides, with three fatty acid chains, are the most suitable for green diesel production, typically involving oxygen removal to form alkanes. Diglycerides, which accounted for 38.77%, also contribute to green diesel, though less efficiently. They are often intermediates formed during partial hydrolysis of triglycerides or thermal cracking, and their presence may indicate incomplete conversion during earlier processing steps (Nenyoo et al., 2024). Nevertheless, diglycerides retain two fatty acid chains, making them valuable for hydrocarbon production (Zhou et al., 2023).

Monoglycerides, present in smaller amounts, are intermediates that convert into glycerol and free fatty acids before further hydrocarbon formation. Their limited presence suggests that most of the feedstock remained in the more energy-dense triglyceride and diglyceride forms (Kordouli *et al.*, 2017). The relatively high diglyceride fraction implies partial hydrolysis, a common pre-treatment stage in green diesel production (Serrano *et al.*, 2021). In some processes, catalysts such as sulfided Co–Mo or Ni–Mo are used to promote HDO of triglycerides and diglycerides into paraffinic hydrocarbons (Peters *et al.*, 2024). Overall, the dominance of triglycerides is favorable for green diesel production, while diglycerides also enhance output, though monoglycerides may point to a need for optimized pre-treatment and reaction conditions.

## 3.2 Catalyst Characterization

The marble analyzed as a catalyst support for WCO deoxygenation contained various oxides that could influence the reaction. X-ray fluorescence (XRF) analysis revealed that CaO was the dominant oxide (35.4%), confirming the calciterich nature of marble (Table 3). The high CaO content indicates strong potential for use as a catalyst support, as CaO enhances reactivity and thermal stability. CaO also contributes to deoxygenation by promoting triglyceride and fatty acid conversion through cracking and DCO<sub>2</sub> mechanisms. Other oxides, including  $Al_2O_3$  and  $SiO_2$ , provide additional stability and improve the dispersion of active metals on the catalyst surface, enhancing reaction efficiency (Han *et al.*, 2015). Based on its oxide composition, marble waste is a promising support material when combined with optimal operating conditions

**Table 3**Marble Waste Characterization

warbie waste Characterization				
Compound	Mass (%)			
MgO	2.06			
$Al_2O_3$	1.63			
$SiO_2$	7.15			
$P_2O_5$	0.108			
SO <sub>3</sub>	0.061			
$K_2O$	0.301			
CaO	35.4			
$TiO_2$	0.164			
MnO	0.0431			
$Fe_2O_3$	1.43			

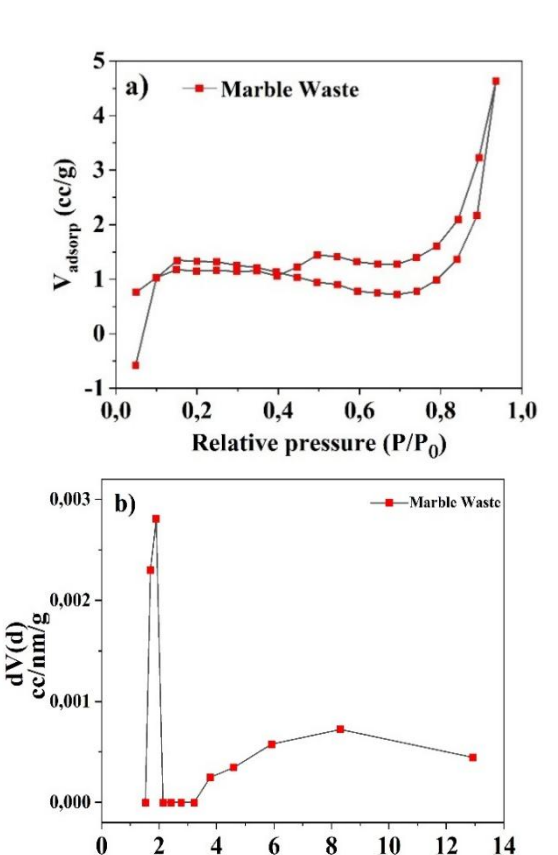


Fig 2.  $N_2$  adsorption-desorption isotherms (a) and pore size distributions by the Density Functional Theory (DFT) method (b) of the marble waste

Pore width (nm)

such as temperature and pressure. Previous studies have shown that oxide-based catalysts, including CaO, Al<sub>2</sub>O<sub>3</sub>, and SiO<sub>2</sub>, are effective for deoxygenation, producing long-chain hydrocarbons that form the main fraction of green diesel (Kaewmeesri *et al.*, 2020).

Surface textural properties were characterized using N2 adsorption-desorption at liquid nitrogen temperature. The marble waste catalyst and the pore size distribution are shown in Fig. 2. The marble waste powder is a non-porous material exhibiting a type II isotherm, typical of non-porous calcite and dolomite minerals. It showed a surface area of 3.81 m<sup>2</sup>/g, a pore volume of 0.006 cm<sup>3</sup>/g, and an average pore diameter of 3.79 nm. XRD analysis was conducted to identify crystalline phases in raw marble waste and the 10% Ni/marble waste catalyst (Fig. 3). Raw marble diffraction patterns showed dominant calcite peaks (CaCO<sub>3</sub>) [JCPDS 05-0586] at  $2\theta = 29.4^{\circ}$ ,  $39.4^{\circ}$ , and  $47.5^{\circ}$ , with minor quartz (SiO<sub>2</sub>) [JCPDS 46-1045] and dolomite (CaMg(CO<sub>3</sub>)<sub>2</sub>) [JCPDS 36-0426]. After nickel impregnation, new peaks appeared at  $2\theta = 37.2^{\circ}$  and  $43.3^{\circ}$ , corresponding to NiO (JCPDS 47-1049), confirming successful deposition of Ni on the marble surface.

## 3.3 Statistical Analysis and Empirical Models for Waste Cooking Oil

The experimental design and results from the Box-Behnken approach are summarized in Table 4, showing the effects of

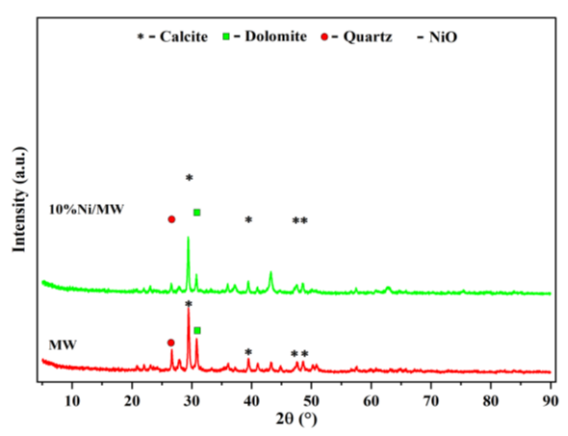


Fig 3. XRD pattern of marble waste and Ni/Marble waste

reaction time, temperature, and catalyst weight on conversion. The outcomes of WCO deoxygenation, based on the Statistica 6.0 analysis, are presented in Table 5.

The regression analysis employed second-order polynomial equations to explain the correlation between independent and dependent variables. The polynomial equation is presented as follows.

$$Y = -2383.50 + 4.862 X_1 + 13.267 X_2 - 0.09835 X_3 - 0.4030 X_1^2 - 0.01778 X_2^2 + 0.4277 X_3^2 + 0.004303 X_1X_2 + 0.0748 X_1X_3 - 0.00612 X_2X_3$$
 (5)

#### Where:

Y: Percentage of WCO Conversion (%)

X<sub>1</sub>: Reaction Time (hour)

X<sub>2</sub>: Reaction Temperature (°C)

X<sub>3</sub>: Catalyst Weight (% w/w)

The polynomial equation indicates that the variables significantly influenced WCO conversion, as shown by the positive constant values in the model. Positive signs of certain terms reflected synergistic effects, while negative signs indicated antagonistic effects. Thus,  $X_1$ ,  $X_2$ ,  $X_3$ , and the interaction between  $X_1$  and  $X_2$  had notable effects on WCO conversion. In contrast, the square terms  $(X_1^2, X_2^2, X_3^2)$  and the interactions  $X_1X_3$  and  $X_2X_3$  showed limited influence. The linear effects suggest that conversion increased with reaction time, temperature, and catalyst concentration, whereas the quadratic and some interaction terms had adverse effects, indicating a potential decrease in conversion under specific conditions.

**Table 4**Experimental Design Using Box-Behnken Design

		Variable		_
Run	Time (Hour)	Temperature (°C)	Catalyst Weight (% w/w)	Response (%)
1	2.0	360	3.0	86.81
2	6.0	360	3.0	87.82
3	2.0	380	3.0	89.39
4	6.0	380	3.0	90.04
5	2.0	370	1.0	93.19
6	6.0	370	1.0	93.97
7	2.0	370	6.0	91.09
8	6.0	370	6.0	93.27
9	4.0	360	1.0	91.62
10	4.0	380	1.0	91.99
11	4.0	360	6.0	93.54
12	4.0	380	6.0	93.71
13	4.0	370	3.0	92.05
14	4.0	370	3.0	91.96
15	4.0	370	3.0	91.70

The ANOVA results confirmed the adequacy of the regression model, with an F-value of 4.18 and a p-value of 0.0649, slightly above the 0.05 threshold. This outcome suggests moderate significance, meaning the model captured meaningful variance despite not being strongly significant. Among the interaction terms,  $X_2X_3$  (temperature × catalyst weight) had the most substantial effect (F = 15.83, p = 0.0105), while  $X_1X_3$  (time × catalyst weight) also showed significance (F = 7.75, p = 0.0387). These findings indicate that optimizing reaction parameters in combination is more effective than adjusting them individually.

In ANOVA, p-values help determine statistical significance. A p-value less than 0.05 indicates a 95% confidence level, meaning the variable significantly affects the response (Ameen *et al.*, 2020). In this study, the linear and quadratic terms of reaction time  $(X_1)$  and reaction temperature  $(X_2)$  were statistically significant, as their p-values were below 0.05.

The lack-of-fit test produced a p-value of 0.0129, suggesting that the quadratic model did not fully account for variability in the experimental data. This result points to a statistically significant lack of fit, possibly due to nonlinear or higher-order interactions beyond a second-order polynomial. Additionally, the relatively small number of center-point replicates (n = 3)

ANOVA Results for the Quadratic Equation Model in the Deoxygenation of Waste Cooking Oil

Source	Df	SS	MS	p-value	F-value
Model	9	56.71	6.3011128423912	0.0649	4.17827855825
$X_1$	1	2.98	2.9765743818662	0.2190	1.9737714952694
$X_2$	1	3.37	3.3676832271551	0.1953	2.2331164305352
$X_3$	1	0.0894	0.089365276130593	0.8173	0.059258265396632
$X_{1}^{2}$	1	0.0296	0.029619083020577	0.8940	0.01964046393001
$X_{2}^{2}$	1	0.5712	0.57121892888432	0.5652	0.37877623561462
$X_{3}^{2}$	1	0.0957	0.095733291743414	0.8111	0.063480907294846
$X_1X_2$	1	9.60	9.5951795834619	0.0530	6.3625797726426
$X_1X_3$	1	11.68	11.68357455763	0.0387	7.7473980039585
$X_2X_3$	1	23.87	23.868726414107	0.0105	15.827392761142
Residual	5	7.54	1.5080643271018		
Lack-of-Fit	3	7.48	2.4917795138175	0.0129	76.690085321194
$R^2 = 0.87162$					

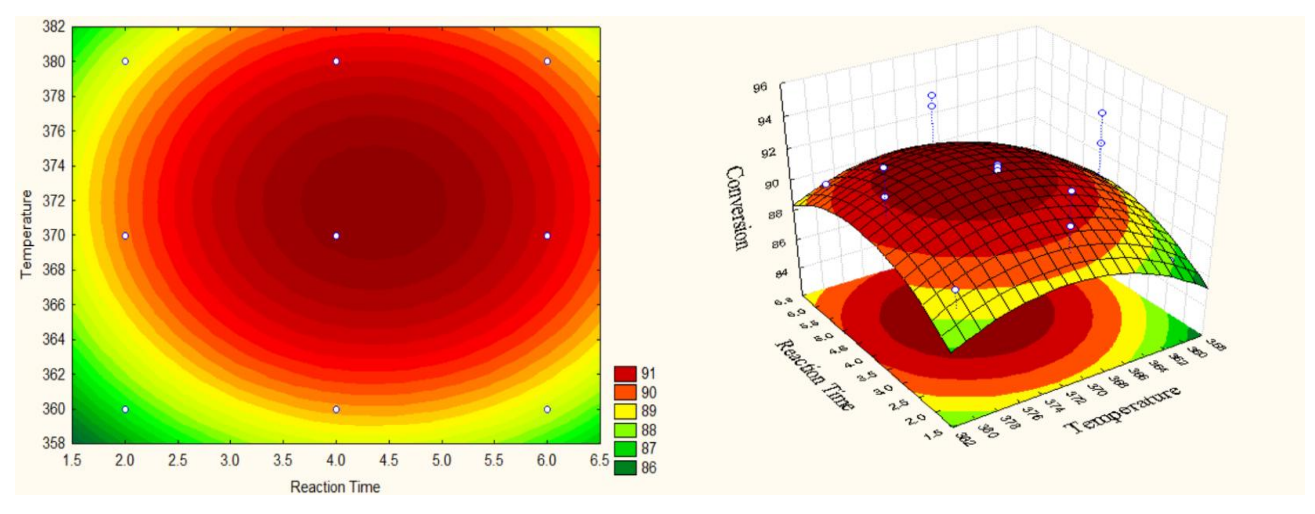


Fig 4. Response surface effect of the deoxygenation process

may have limited the statistical power to detect subtle inadequacies.

While the model provided a strong approximation within the tested experimental range ( $R^2 = 87.16\%$ ), caution is advised when extrapolating beyond these conditions. Improvements such as increasing replicates or incorporating higher-order models (e.g., cubic terms or neural networks) could enhance predictive accuracy and reduce lack of fit. Overall, the empirical model captured the dominant effects and interactions of reaction time, temperature, and catalyst weight on WCO conversion, though predictive performance remains constrained by the identified lack of fit.

# 3.4 Optimization of Green Diesel from Waste Cooking Oil through Deoxygenation using Response Surface Methodology

After model evaluation, response plots in the form of surfaces and contours were used to determine optimal values. Three-dimensional (3-D) response surface and contour plots, derived from the regression equation (Eq. 5), illustrated the relationship between responses and experimental variables. These plots also revealed the nature of interactions between pairs of variables. As shown in Fig. 4, which depicts the combined effects of reaction time and temperature on WCO conversion during deoxygenation, the highest conversion values were concentrated in the central region, corresponding to intermediate reaction times and moderate-to-high temperatures. Table 6 shows that the optimum conditions are at a temperature of 373.64 °C, a residence time of 4.35 hours, and a catalyst loading of 3.45% w/w.

The response surface plots indicate that the percentage of WCO conversion increased with reaction time, reaction temperature, and catalyst weight, up to a certain critical point. The highest percentage of WCO conversion is represented in the contour plot area in solid red, while the lowest conversion

percentage is shown in green. Increased temperature improved solubility and diffusion coefficients, enhancing conversion. The 3-D response surface and contour plots provide insights into the interaction effects of the independent variables on WCO conversion. The curved and nonlinear shapes of the response surfaces suggest significant interaction and quadratic effects. The surface between reaction time and temperature showed a rising ridge, indicating a synergistic interaction where increasing both parameters simultaneously conversion yield up to an optimum point. The interaction between reaction temperature and catalyst weight displayed a slightly concave curvature, implying that while temperature had a strong effect, increasing catalyst loading beyond a certain point did not linearly increase conversion and might level off due to diffusion limitations or pore saturation. The 3-D surface plot reinforces these observations, showing pronounced curvature that highlights the strong interactive effect between temperature and reaction time. This indicates diminishing returns at higher operating conditions and confirms the existence of an optimum rather than a linear improvement. These shapes validate the statistical findings from ANOVA and confirm that the system's behavior involved more than just additive effects, highlighting the importance of simultaneous optimization of variables.

The results of the desirability function analysis for each independent variable and the predicted response under optimal conditions are shown in the desirability profile. The graph indicates that WCO conversion in deoxygenation using Ni/marble increased with reaction time, temperature, and catalyst weight until they reached critical values. Excessive catalyst quantities or insufficient reaction time might hinder conversion due to limited interaction between reactants and active sites. Catalyst overload can also lead to coke formation and pore blockage (Onlamnao *et al.*, 2020). This combination is consistent with the deoxygenation of triglycerides, sufficient to

**Table 6**Ontimum Process of Deoxygenation of Waste Cooking Oil

Optimum rocess of Deoxygenation	ii oi waste cookiiig t	J11			
Variable	Code		Parametric		
		Min	Opt	Max	
Reaction Time (hour)	$X_1$	2	4.35	6	
Reaction Temperature (°C)	$X_2$	360	373.64	380	
Catalyst Weight (% w/w)	$X_3$	1	3.45	6	

drive hydrodeoxygenation, decarboxylation, and decarbonylation while avoiding excessive thermal cracking that produces light gases and reduces liquid yield. Under these conditions, the optimum WCO conversion was 93.56%.

## 3.5 Product Distribution Analysis

The catalytic performance of the Ni/marble waste catalyst was evaluated in a deoxygenation reaction with a constant nitrogen flow rate of 0.5 mL/min, with variables shown in Table 4. The WCO used consisted of monoglycerides (3.05%), diglycerides (38.77%), and triglycerides (58.17%).

Fig. 5 shows the optimum product distribution from the deoxygenation of WCO. Peaks were observed in the retention time range of C15–C18 hydrocarbons, corresponding to the major fatty acid chains listed in Table 2. This confirms that the deoxygenation pathways successfully removed oxygenated groups and converted triglycerides and FFAs into long-chain paraffins suitable for green diesel.

The predominant peaks corresponded to n-paraffins and iso-paraffins with carbon numbers mainly between C15 and C18, which fall within the diesel boiling range. Thus, the optimized reaction conditions led to selective production of diesel-like hydrocarbons. The yield of green diesel consistently dominated over gasoline and kerosene. For certain variables, such as the 3rd and 10th, the green diesel yield remained above 60%, indicating stable production. Kerosene yields were lower than diesel but higher than gasoline in most cases, reflecting focus on medium-chain hydrocarbons. A noticeable increase in kerosene yield was observed for the 9th and 12th variables, suggesting that temperature or catalyst weight promoted medium-chain hydrocarbon production under certain conditions (Goh *et al.*, 2023).

Selectivity followed similar patterns. Green diesel selectivity was consistently high, showing effective conversion to long-chain hydrocarbons. Kerosene selectivity fluctuated, with peaks in the 9th and 12th variables, suggesting greater selectivity toward medium-chain hydrocarbons under specific conditions. This behavior can be attributed to the CaO-rich marble support, which acts as a strong basic catalyst favoring DCO<sub>2</sub> and DCO reactions that remove COOH and CO groups as CO<sub>2</sub> or CO (Papageridis *et al.*, 2020). Marble also provides good thermal stability and surface area, supporting even distribution of Ni particles.

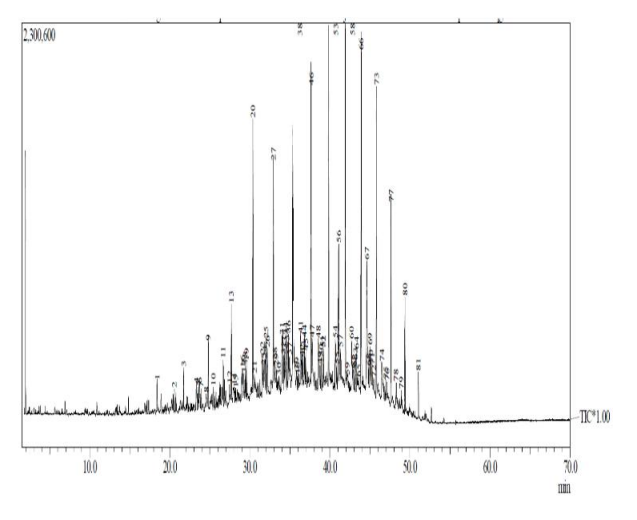


Fig 5. Optimum product deoxygenation process

Nickel facilitated hydrogenation of fatty acids and triglycerides into alcohols or alkenes, with oxygen removed as  $H_2O$ , thus increasing the yield of long-chain hydrocarbons (C12–C20) suitable for diesel (Zhong *et al.*, 2021). Ni also enabled HDO, DCO, and DCO<sub>2</sub> by activating hydrogen and cleaving C–O and C–C bonds. Its surface adsorbed and dissociated reactants effectively, showing catalytic properties similar to noble metals like Pd and Pt. The performance of Ni depended on support characteristics such as surface area, acidity, and pore structure, which affected Ni dispersion and activity (Riyandi *et al.*, 2024).

The product distribution resulting from the deoxygenation of waste cooking oil is illustrated in Fig. 6, which classifies the hydrocarbon products into paraffins, olefins, and aromatics. Across all runs, paraffins dominated, confirming that deoxygenation effectively converted triglycerides and FFAs into saturated hydrocarbons suitable for green diesel. This outcome is consistent with decarboxylation, decarbonylation, and hydrodeoxygenation pathways, which predominantly yield linear and branched alkanes in the C15–C18 range.

The process began with thermal cleavage of triglycerides, releasing palmitic, oleic, and stearic acids. These underwent decarboxylation and decarbonylation, producing hexadecane and octadecane within the diesel range. The main pathway was HDO, with oxygen removed as water in the presence of hydrogen. DCO2 and DCO contributed but mainly produced lighter fractions such as kerosene and gasoline (Gousi et al., 2017). For instance, Istadi et al. (2023) reported a Co-Ni/ZSM-5 catalyst achieving 76.5% triglyceride conversion, yielding 2.61% gasoline, 4.38% kerosene, and 61.75% diesel. Ni<sub>2</sub>P/Al-SBA-15 also showed strong deoxygenation performance, with DCO<sub>2</sub> and DCO as the dominant routes in oleic acid conversion (Camargo et al., 2020). The strong basicity of CaO further enhanced diesel selectivity by removing oxygen as CO2 and CO, without requiring high-surface-area synthetic supports (Chueaphetr et al., 2023).

Similarly, the importance of metal dispersion, reducibility, and nickel active site density has been emphasized with Ni/MgO-Al<sub>2</sub>O<sub>3</sub> catalysts. Their optimal configuration (20 wt.% Ni) achieved the highest activity due to greater hydrogenation capacity and enhanced oxygen removal via HDO (Jeon *et al.*, 2022). These findings are consistent with previous reports showing that well-dispersed nickel on thermally stable marble support provided efficient catalytic performance in HDO, removing oxygen as water and improving the formation of diesel-range long-chain hydrocarbons. The reaction mechanism

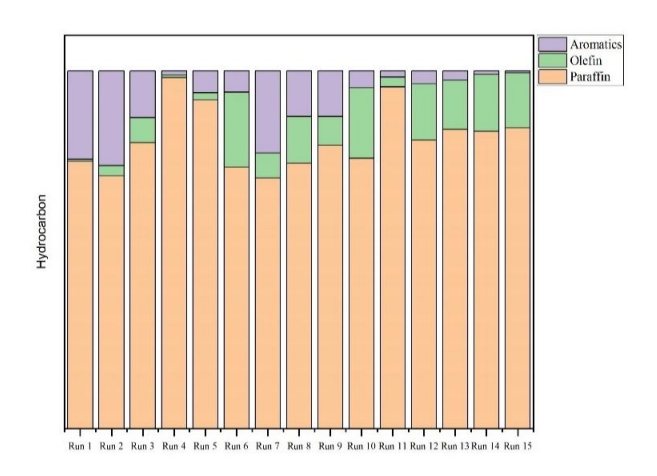


Fig 6. Product distribution analysis of the deoxygenation of the product

was found to proceed mainly through decarboxylation of fatty aldehydes, with HDO and DCO<sub>2</sub> acting as secondary pathways and contributing marginally to product distribution.

#### 3.6 Reaction Mechanism

The proposed reaction pathway was elucidated from the product distribution and chemical composition of the liquid hydrocarbons, as determined by GC–MS analysis. Under thermal cracking conditions, waste cooking oil (WCO), consisting of mono-, di-, and triglycerides, underwent molecular fragmentation to form oxygenated intermediates. Subsequent deoxygenation reactions, facilitated by the Ni/marble waste catalyst, occurred predominantly on the catalyst's external surface, generating heavy hydrocarbons. The main products identified, such as hexadecane ( $C_{16}H_{34}$ ), heptadecane ( $C_{17}H_{36}$ ), and octadecane ( $C_{18}H_{38}$ ), contained no oxygenated functional groups, confirming effective oxygen removal.

The reaction pathways for WCO deoxygenation, illustrated in Fig. 7, show how triglycerides are transformed into hydrocarbon fuels. WCO, mainly composed of triglycerides with palmitic, stearic, and oleic acids, undergoes a series of thermal and catalytic reactions in the presence of the Ni/marble catalyst. In the deoxygenation mechanism, oxygen is removed from fatty acids and triglycerides without external hydrogen, producing H<sub>2</sub>O, CO<sub>2</sub>, and CO as by-products (Prangklang *et al.*, 2023). The catalyst was essential in facilitating these reactions, yielding saturated hydrocarbons free from oxygen. The mechanism begins with thermal decomposition of triglycerides into free fatty acids such as palmitic acid (C16:0), stearic acid (C18:0), and oleic acid (C18:1). These acids then undergo DCO<sub>2</sub>, DCO, and HDO reactions (Serrano *et al.*, 2021).

Palmitic and stearic acids were converted into hexadecane and octadecane via DCO, with  $CO_2$  released. For unsaturated fatty acids like oleic acid, DCO produced heptadecane, CO, and  $H_2O$ . The DCO $_2$  and DCO reactions efficiently eliminated oxygen, forming fully saturated hydrocarbons (Nikolopoulos *et al.*, 2023). At the same time, the water–gas shift (WGS) reaction generated hydrogen in situ, as CO reacted with  $H_2O$  to produce  $CO_2$  and  $H_2$ . Hydrogen was subsequently used in transfer hydrogenation, promoting further conversion of intermediates into lighter alkenes (Oi *et al.*, 2020).

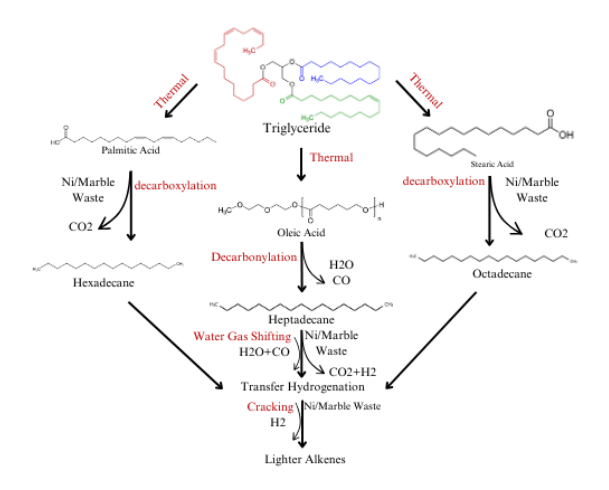


**Fig 7.** Possible reaction of waste cooking oil into fuel by deoxygenation Process

Nickel effectively catalyzed these deoxygenation reactions by lowering activation energy for bond cleavage (Shi *et al.*, 2023). Marble waste (CaCO<sub>3</sub>) served as a support, dispersing nickel particles and stabilizing the catalyst at high temperatures. This ensured selective conversion of esters and fatty acids into hydrocarbons while minimizing by-products. The GC–MS results confirmed efficient deoxygenation, with hexadecane, octadecane, and heptadecane identified as dominant end products. These hydrocarbons, with high energy content and compatibility with diesel, are highly suitable as biofuels.

Under optimum conditions, the main products—octadecane and heptadecane—showed no oxygen-containing groups, confirming HDO had occurred. In this process, O<sub>2</sub> was removed by hydrogen, producing H<sub>2</sub>O as the by-product. Supported nickel catalysts are especially effective in this pathway, yielding fully saturated hydrocarbons for diesel (Hongloi et al., 2022). The hydrocarbons detected by GC–MS, including hexadecane, octadecane, and heptadecane, highlight the catalyst's efficiency. These profiles align with earlier studies showing nickel catalysts effectively convert fatty acid derivatives, especially esters, into long-chain alkanes via deoxygenation and decarboxylation (Lycourghiotis *et al.*, 2021).

#### 3.7 Economic Analysis

Economic viability must also be considered to determine feasibility and competitiveness with conventional fuels. Technoeconomic analysis helps identify the commercial potential of products from the designed process. Biofuel production from WCO using the Ni/marble waste catalyst showed significant economic benefits, primarily due to low-cost, sustainable raw materials. The analysis was based on reaction temperature, reaction time, and catalyst weight at optimum process conditions.

The economic feasibility was further assessed by evaluating variable operating costs (Table 7). The total variable cost was \$0.1710 per batch, dominated by electricity. With consumption of 0.9533 kWh at \$0.0953 per kWh, electricity represented the largest share of costs. This emphasizes the importance of energy efficiency in optimizing economics. The catalyst achieved a 91.3% conversion of WCO to hydrocarbons. At 373.64 °C and 4.35 h, energy use was significantly lower than in high-temperature cracking, reducing costs per unit through free-hydrogen deoxygenation. Assumptions for the evaluation are summarized in Table 8. Indonesia was chosen as the plant

**Table 7**The List of Variable Operating Costs

The List of Variable Operating Costs				
Variable	Consumption	Unit Cost (US\$		
		Per Unit)		
Feedstock WCO	0.1247 L	0.0523		
Marble Waste	0.00556 kg	0.00269		
Catalyst				
Inert gas (N <sub>2</sub> )	$0.0005 \text{ m}^3$	0.0000215		
Electricity	0.9533 kWh	0.0953		
	Total	0.1710		

**Table 8**The Assumptions Used in the Economic Analysi

	The Assumptions Osed in the Economic Analysis				
Assumptions					
	Location of Plant	Indonesia			
	Lifetime of Plant	10 Years			
	Operational of Plant	4 batches/day			
	Depreciation	0.5 TCI			

Table 9

Profitability Metrics			
Metrics	Value		
Operating Cost	\$256.50		
Revenue	\$7,396.59		
Net Profit	\$7,140.09		
Return on Investment	72.80%		
Payback Period	0.70 Years		
Net Present Value	\$38,353.91		
Internal Rate of Return	79.33%		

location, reflecting the abundance of WCO and marble waste. The plant lifetime was assumed at 10 years, consistent with design horizons for small- to medium-scale chemical plants.

Profitability analysis (Table 9) showed the process is economically viable with strong indicators. Operating costs of \$256.50 compared to revenue of \$7,396.59 yielded a net profit of \$7,140.09 per cycle, demonstrating cost-effectiveness from using WCO and marble waste. The return on investment (ROI) was 72.80%, much higher than conventional biofuel production, and supported by a payback period of only 0.70 years. This indicates capital investment could be recovered in less than one year. Revenue from biofuel sales was estimated at \$1.25 per liter (Hsu et al., 2021). With a yield of 0.9743 liters, the profit per batch was \$1.0469. These results suggest biofuel production from WCO is profitable, although electricity and nitrogen costs should be monitored for optimization. The system is economically viable even at laboratory scale. The use of inexpensive raw materials, coupled with ambient-pressure deoxygenation and no need for external hydrogen, further enhances cost-effectiveness compared to hydrotreatment technologies.

## Acknowledgment

The authors express their sincere gratitude to the Indonesia Collaboration Research (*RKI*) Program for their support, with grant contract number 391-18/UN7.D2/PP/V/2023.

## References

- Aliana-Nasharuddin, N., Asikin-Mijan, N., Abdulkareem-Alsultan, G., Saiman, M. I., Alharthi, F. A., Alghamdi, A. A., & Taufiq-Yap, Y. H. (2019). Production of green diesel from catalytic deoxygenation of chicken fat oil over a series binary metal oxide-supported MWCNTs. *RSC Advances*, *10*(2), 626–642. https://doi.org/10.1039/c9ra08409f
- Ameen, M., Azizan, M. T., Yusup, S., Ramli, A., Shahbaz, M., & Aqsha, A. (2020). Process optimization of green diesel selectivity and understanding of reaction intermediates. *Renewable Energy, 149*, 1092–1106. https://doi.org/10.1016/j.renene.2019.10.108
- Asikin-Mijan, N., Lee, H. V., Taufiq-Yap, Y. H., Juan, J. C., & Rahman, N. A. (2016). Pyrolytic-deoxygenation of triglyceride via natural waste shell derived Ca(OH)2 nanocatalyst. *Journal of Analytical and Applied Pyrolysis*, 117, 46–55. https://doi.org/10.1016/j.jaap.2015.12.017
- Chiaramonti, D., Buffi, M., Rizzo, A. M., Lotti, G., & Prussi, M. (2016).

  Bio-hydrocarbons through catalytic pyrolysis of used cooking oils and fatty acids for sustainable jet and road fuel production.

  Biomass and Bioenergy, 95, 424–435. https://doi.org/10.1016/j.biombioe.2016.05.035
- Choo, M. Y., Oi, L. E., Ling, T. C., Ng, E. P., Lin, Y. C., Centi, G., & Juan, J. C. (2020). Deoxygenation of triolein to green diesel in the H2-free condition: Effect of transition metal oxide supported on zeolite Y. Journal of Analytical and Applied Pyrolysis,

- 147(February), 104797. https://doi.org/10.1016/j.jaap.2020.104797
- Chueaphetr, R., Suwannaruang, T., Khunphonoi, R., Khemthong, P., & Wantala, K. (2023). Enhancing deoxygenation of waste cooking palm oil over CaO-MgO catalyst modified by K2O for green biofuel. *Fuel*, *354*(February), 129350. https://doi.org/10.1016/j.fuel.2023.129350
- de Oliveira Camargo, M., Castagnari Willimann Pimenta, J. L., de Oliveira Camargo, M., & Arroyo, P. A. (2020). Green diesel production by solvent-free deoxygenation of oleic acid over nickel phosphide bifunctional catalysts: Effect of the support. *Fuel*, 281(April), 118719. https://doi.org/10.1016/j.fuel.2020.118719
- Di Vito Nolfi, G., Gallucci, K., Mucciante, V., & Rossi, L. (2025).

  Production of Green Diesel via the Ni/Al Mo Hydrotalcite
  Catalyzed Deoxygenation of Rapeseed Oil. *Molecules*, 30(8), 1–23.

  https://doi.org/10.3390/molecules30081699
- Doliente, S. S., Narayan, A., Tapia, J. F. D., Samsatli, N. J., Zhao, Y., & Samsatli, S. (2020). Bio-aviation Fuel: A Comprehensive Review and Analysis of the Supply Chain Components. *Frontiers in Energy Research*, *8*(July), 1–38. https://doi.org/10.3389/fenrg.2020.00110
- Febriansyar, R. A., Riyanto, T., Istadi, I., Anggoro, D. D., & Jongsomjit, B. (2023). Bifunctional CaCO3/HY Catalyst in the Simultaneous Cracking-Deoxygenation of Palm Oil to Diesel-Range Hydrocarbons. *Indonesian Journal of Science and Technology*, 8(2), 281–306. https://doi.org/10.17509/ijost.v8i2.55494
- Goh, B. H. H., Chong, C. T., & Ng, J. H. (2023). Hydrogen-free Deoxygenation of Waste Cooking Oil over Unreduced Bimetallic NiCo Catalysts for Biojet Fuel Production. *Chemical Engineering Transactions*, 106(August), 721–726. https://doi.org/10.3303/CET23106121
- Gousi, M., Andriopoulou, C., Bourikas, K., Ladas, S., Sotiriou, M., Kordulis, C., & Lycourghiotis, A. (2017). Green diesel production over nickel-alumina co-precipitated catalysts. *Applied Catalysis A: General*, 536, 45–56. https://doi.org/10.1016/j.apcata.2017.02.010
- Hafriz, R. S. R. M., Salmiaton, A., Yunus, R., & Taufiq-Yap, Y. H. (2018). Green Biofuel Production via Catalytic Pyrolysis of Waste Cooking Oil using Malaysian Dolomite Catalyst. *Bulletin of Chemical Reaction Engineering and Catalysis*, 13(3), 489–501. https://doi.org/10.9767/bcrec.13.3.1956.489-501
- Hafriz, R. S. R. M., Shafizah, I. N., Arifin, N. A., Salmiaton, A., Yunus, R., Yap, Y. H. T., & Shamsuddin, A. H. (2021). Effect of Ni/Malaysian dolomite catalyst synthesis technique on deoxygenation reaction activity of waste cooking oil. *Renewable Energy*, 178, 128–143. https://doi.org/10.1016/j.renene.2021.06.074
- Han, F., Guan, Q., & Li, W. (2015). Deoxygenation of methyl palmitate over SiO2-supported nickel phosphide catalysts: effects of pressure and kinetic investigation. RSC Advances, 5(130), 107533– 107539. https://doi.org/10.1039/c5ra22973a
- Hongloi, N., Prapainainar, P., & Prapainainar, C. (2022). Review of green diesel production from fatty acid deoxygenation over Ni-based catalysts. *Molecular Catalysis*, 523(January 2021), 111696. https://doi.org/10.1016/j.mcat.2021.111696
- Hsu, H., Chang, Y., & Wang, W. (2021). Techno-economic analysis of used cooking oil to jet fuel production under uncertainty through three-, two-, and one-step conversion processes. *Journal of Cleaner Production*, 289, 125778. https://doi.org/10.1016/j.jclepro.2020.125778
- Istadi, I., Riyanto, T., Anggoro, D. D., Pramana, C. S., & Ramadhani, A. R. (2023). High Acidity and Low Carbon-Coke Formation Affinity of Co-Ni/ZSM-5 Catalyst for Renewable Liquid Fuels Production through Simultaneous Cracking-Deoxygenation of Palm Oil. Bulletin of Chemical Reaction Engineering and Catalysis, 18(2), 222–237. https://doi.org/10.9767/bcrec.17974
- Jeon, K. W., Park, H. R., Lee, Y. L., Kim, J. E., Jang, W. J., Shim, J. O., & Roh, H. S. (2022). Deoxygenation of non-edible fatty acid for green diesel production: Effect of metal loading amount over Ni/MgO-Al2O3 on the catalytic performance and reaction pathway. Fuel, 311(November 2021), 122488. https://doi.org/10.1016/j.fuel.2021.122488
- Kaewmeesri, R., Nonkumwong, J., Witoon, T., Laosiripojana, N., & Faungnawakij, K. (2020). Effect of water and glycerol in deoxygenation of coconut oil over bimetallic nico/sapo-11

- nanocatalyst under n2 atmosphere. *Nanomaterials*, 10(12), 1–15. https://doi.org/10.3390/nano10122548
- Kordouli, E., Sygellou, L., Kordulis, C., Bourikas, K., & Lycourghiotis, A. (2017). Probing the synergistic ratio of the NiMo/Γ-Al2O3 reduced catalysts for the transformation of natural triglycerides into green diesel. *Applied Catalysis B: Environmental*, 209, 12–22. https://doi.org/10.1016/j.apcatb.2017.02.045
- Krobkrong, N., Itthibenchapong, V., Khongpracha, P., & Faungnawakij, K. (2018). Deoxygenation of oleic acid under an inert atmosphere using molybdenum oxide-based catalysts. *Energy Conversion and Management*, 167(April), 1–8. https://doi.org/10.1016/j.enconman.2018.04.079
- Kubicka, D. (2019). Upgrading of lipids to hydrocarbon fuels via (hydro)deoxygenation. *Chemical Catalysts for Biomass Upgrading*, 469–496. https://doi.org/10.1002/9783527814794.ch11
- Lycourghiotis, S., Kordouli, E., Kordulis, C., & Bourikas, K. (2021).

  Transformation of residual fatty raw materials into third generation green diesel over a nickel catalyst supported on mineral palygorskite. *Renewable Energy*, 180, 773–786. https://doi.org/10.1016/j.renene.2021.08.059
- Mulyatun, M., Istadi, I., & Widayat, W. (2023). Synthesis and Characterization of Physically Mixed V2O5.CaO as Bifunctional Catalyst for Methyl Ester Production from Waste Cooking Oil. International Journal of Renewable Energy Development, 12(2), 381–389. https://doi.org/10.14710/ijred.2023.51047
- Nenyoo, P., Wongsurakul, P., Kiatkittipong, W., Kaewtrakulchai, N., Srifa, A., Eiad-Ua, A., & Assabumrungrat, S. (2024). Catalytic Deoxygenation of Palm Oil Over Iron Phosphide Supported on Nanoporous Carbon Derived from Vinasse Waste for Green Diesel Production. ACS Omega. https://doi.org/10.1021/acsomega.4c05000
- Nikolopoulos, I., Kogkos, G., Tsavatopoulou, V. D., Kordouli, E., Bourikas, K., Kordulis, C., & Lycourghiotis, A. (2023). Nickel— Alumina Catalysts for the Transformation of Vegetable Oils into Green Diesel: The Role of Preparation Method, Activation Temperature, and Reaction Conditions. *Nanomaterials*, 13(3). https://doi.org/10.3390/nano13030616
- Oi, L. E., Choo, M. Y., Lee, H. V., Taufiq-Yap, Y. H., Cheng, C. K., & Juan, J. C. (2020). Catalytic deoxygenation of triolein to green fuel over mesoporous TiO2 aided by in situ hydrogen production. *International Journal of Hydrogen Energy*, 45(20), 11605–11614. https://doi.org/10.1016/j.ijhydene.2019.07.172
- Onlamnao, K., Phromphithak, S., & Tippayawong, N. (n.d.). P a g e | Generating Organic Liquid Products from Catalytic Cracking of Used Cooking Oil over Mechanically Mixed Catalysts. *Journal of Renewable Energy Development*, 9(2), 159–166. https://doi.org/10.14710/ijred.9.2.157-166
- Papageridis, K. N., Charisiou, N. D., Douvartzides, S., Sebastian, V., Hinder, S. J., Baker, M. A., AlKhoori, S., Polychronopoulou, K., & Goula, M. A. (2020). Promoting effect of CaO-MgO mixed oxide on Ni/γ-Al2O3 catalyst for selective catalytic deoxygenation of palm oil. *Renewable Energy*, 162, 1793–1810. https://doi.org/10.1016/j.renene.2020.09.133
- Peters, M. A., Onwudili, J. A., & Wang, J. (2024). Fuel-range liquid hydrocarbon products from catalytic deoxygenation of mixtures of fatty acids obtained from the hydrolysis of rapeseed oil. Sustainable Energy & Fuels. https://doi.org/10.1039/d4se00864b

- Prangklang, D., Tumnantong, D., Yoosuk, B., Ngamcharussrivichai, C., & Prasassarakich, P. (2023). Selective Deoxygenation of Waste Cooking Oil to Diesel-Like Hydrocarbons Using Supported and Unsupported NiMoS2 Catalysts. ACS Omega, 8(43), 40921–40933. https://doi.org/10.1021/acsomega.3c06188
- Reza, M. S., Zhanar Baktybaevna, I., Afroze, S., Kuterbekov, K., Kabyshev, A., Bekmyrza, K. Z., Kubenova, M. M., Bakar, M. S. A., Azad, A. K., Roy, H., & Islam, M. S. (2023). Influence of Catalyst on the Yield and Quality of Bio-Oil for the Catalytic Pyrolysis of Biomass: A Comprehensive Review. *Energies*, 16(14), 1–39. https://doi.org/10.3390/en16145547
- Riyandi, R., Rinaldi, N., Yunarti, R. T., Dwiatmoko, A. A., & Simanjuntak, F. S. H. (2024). Effect of various silica-supported nickel catalyst on the production of bio-hydrocarbons from oleic acid. *International Journal of Renewable Energy Development*, *13*(4), 601–607. https://doi.org/10.61435/ijred.2024.60054
- Scaldaferri, C. A., & Pasa, V. M. D. (2019). Green diesel production from upgrading of cashew nut shell liquid. *Renewable and Sustainable Energy Reviews*, 111(May), 303–313. https://doi.org/10.1016/j.rser.2019.04.057
- Serrano, D. P., Arroyo, M., Briones, L., Hernando, H., & Escola, J. M. (2021). Selective decarboxylation of fatty acids catalyzed by Pdsupported hierarchical ZSM-5 zeolite. *Energy and Fuels*, 35(21), 17167–17181. https://doi.org/10.1021/acs.energyfuels.1c01373
- Shi, F., Wang, H., Chen, Y., Lu, Y., Hou, D., Liu, C., Lu, Y., Lin, X., Yang, X., Zheng, Z., & Zheng, Y. (2023). Green diesel-like hydrocarbon production by H2-free catalytic deoxygenation of oleic acid via Ni/MgO-Al2O3 catalysts: Effect of the metal loading amount. *Journal of Environmental Chemical Engineering*, 11(5), 0–3. https://doi.org/10.1016/j.jece.2023.110520
- Siraj, M., & Ceylan, S. (2025). Investigation of the effect of catalyst support on oleic acid catalytic deoxygenation for green diesel production. *Journal of Porous Materials*, 32(3), 941–952. https://doi.org/10.1007/s10934-024-01725-2
- Sousa, F. P., Silva, L. N., de Rezende, D. B., de Oliveira, L. C. A., & Pasa, V. M. D. (2018). Simultaneous deoxygenation, cracking and isomerization of palm kernel oil and palm olein over beta zeolite to produce biogasoline, green diesel and biojet-fuel. *Fuel*, 223(March), 149–156. https://doi.org/10.1016/j.fuel.2018.03.020
- Sowe, M. S., Lestari, A. R., Novitasari, E., Masruri, M., & Ulfa, S. M. (2022). The Production of Green Diesel Rich Pentadecane (C15) from Catalytic Hydrodeoxygenation of Waste Cooking Oil using Ni/Al2O3-ZrO2 and Ni/SiO2-ZrO2. *Bulletin of Chemical Reaction Engineering and Catalysis*, 17(1), 135–145. https://doi.org/10.9767/BCREC.17.1.12700.135-145
- Zhong, J., Deng, Q., Cai, T., Li, X., Gao, R., Wang, J., Zeng, Z., Dai, G., & Deng, S. (2021). Graphitic carbon embedded FeNi nanoparticles for efficient deoxygenation of stearic acid without using hydrogen and solvent. *Fuel*, 292(February), 120248. https://doi.org/10.1016/j.fuel.2021.120248
- Zhou, Y., Remón, J., Jiang, Z., Matharu, A. S., & Hu, C. (2023). Tuning the selectivity of natural oils and fatty acids/esters deoxygenation to biofuels and fatty alcohols: A review. *Green Energy and Environment*, 8(3), 722–743. https://doi.org/10.1016/j.gee.2022.03.001



© 2025. The Author(s). This article is an open-access article distributed under the terms and conditions of the Creative Commons Attribution-ShareAlike 4.0 (CC BY-SA) International License (http://creativecommons.org/licenses/by-sa/4.0/)